

A Numerical Study of the Fatigue Behaviour of Notched PVD-coated Ti-6Al-4V

S. Baragetti¹ and F. Tordini²

Abstract: The effect of a TiN PVD (Physical Vapor Deposition) coating on the fatigue behaviour of the titanium alloy Ti-6Al-4V was investigated. Fatigue tests were performed on coated and uncoated, both smooth and 120° V-notched, specimens in order to evaluate the influence of the coating on the substrate fatigue resistance. Numerical analyses were carried out in order to determine the stress distributions below the specimen surface and on the coating. Several coating elastic moduli were used in such calculations. The residual stress gradient induced by the coating process deposition and the substrate plasticization were also taken into account with FEM. The numerical analyses were compared to the experimental results in order to interpret them.

Keyword: TiN PVD coatings, residual stresses, V-notch, fatigue, numerical models, submodeling technique.

1 Introduction

Thin hard coatings deposited by means of the PVD technique are used in several mechanical applications [Merlo (2003); Su, Yao, Wei, Kao and Wu (1999); Vetter, Barbezat, Crummenauer and Avissar (2005)]. The surface hardness and wear resistance of the components can be increased by coating deposition. Many research studies dealing with the wear, corrosion and mechanical characterization of different thin coatings are available in the literature [Guu and Hocheng (2001); Mendibide, Steyer, Fontaine and Goudeau (2006); PalDey and Deevi (2003)]. Also, the fatigue resistance of coated components may be enhanced

by some coatings, as a number of studies has demonstrated [Baragetti, La Vecchia and Terranova (2003, 2005); Baragetti (2007); Gelfi, La Vecchia, Lecis and Troglio (2005); Su, Yao, Wei, Wu and Kao (1998)].

Baragetti, La Vecchia and Terranova (2003, 2005) found good results in the fatigue behaviour of duplex stainless steel and H11 tool steel coated with CrN PVD. They also developed a theoretical-numerical model to foresee the number of cycles to failure of thin coated components [Baragetti, La Vecchia and Terranova (2005)]. It is well known that the presence of a surface residual stress field represents one of the main factors affecting the fatigue resistance of mechanical components. The PVD deposition process does induce high residual stresses in the coating and at the substrate surface level. Due to equilibrium requirements, those kinds of stresses clearly have to be self-equilibrated. Their effect can be beneficial to the fatigue resistance in the case of surface compression stresses [Kim, Suh, Murakami and Chung (2003); Su, Yao, Wei, Wu and Kao (1998)] and with an uncracked coating.

For the time being, only few references dealing with the influence of thin hard coatings on the fatigue behaviour of light alloys are available. Such materials are used in many applications, *e.g.* in the automotive and aeronautical industry or in the biomedical field. The possibility of enhancing the mechanical resistance by means of coatings would enable to widen the use of light alloys in advanced and competition applications. Baragetti (2007) studied thin hard coated spur gears. The author found that the presence of a TiN coating improves the fatigue behaviour of both steel and titanium Ti-6Al-4V spur gears. This indicates that the coating deposition could contribute to reduce

¹ Università degli Studi di Bergamo, Bergamo, Italy. E-mail: sergio.baragetti@unibg.it

² Università degli Studi di Ferrara, Ferrara, Italy. E-mail: federico.tordini@unibg.it

the weight of mechanical components, thus enhancing their performances and reducing the fuel consumption.

The Ti-6Al-4V alloy is very attractive for the low weight-to-strength ratio and for its fatigue behaviour, even if its poor wear resistance may require suitable surface treatments, *e.g.* PVD coatings [Wilson, Leyland and Matthews (1999)]. Nevertheless, the study of the influence of such coatings on the fatigue resistance of a Ti-6Al-4V base material still has not been developed enough. In the afore mentioned reference no significant variation in the fatigue behaviour of the TiN PACVD-coated titanium alloy was observed. Kolkman (1995) studied the influence of TiN PVD coatings on the fatigue strength of a Ti-6Al-4V substrate. A significant decrease in the fatigue life occurred with a coating thickness of 50 μm . The author pointed out that the sub-surface tensile residual stresses, which arised to equilibrate the compression ones and were introduced in the surface layer by the deposition process, are highly detrimental to the base material resistance. The effect of the presence of notches in a Ti-6Al-4V alloy is also significant. In [Haritos, Nicholas and Lanning (1999); Lanning, Haritos and Nicholas (1999); Lanning, Nicholas and Haritos (2005)] the notch effect on the high cycle fatigue behaviour was investigated. On the contrary, as far as known to the authors, studies on the combined effect of notches and coating have not been developed yet.

In this work the fatigue behaviour of the titanium alloy Ti-6Al-4V coated by means of TiN PVD arc-deposited hard thin films was studied. Rotating bending tests were carried out on both smooth and notched specimens to evaluate the change occurring in the fatigue resistance of the coated ones [Baragetti, Lusvarghi, Pighetti Mantini and Tordini (2007)]. Several elastic-plastic FE models were processed to evaluate the stress distribution under the surface level of the coated specimens. The numerical results enabled to study the combined effect of the residual stresses induced by the deposition process, and the stress amplification due to the presence of the notch. Moreover, the influence on the stress state of the vari-

ation of the coating elastic modulus was investigated by means of a number of FE models. The stress state data collectable through the analyses could also constitute a suitable input for evaluating the fatigue behaviour of light alloy coated components, by using the Unified Approach developed by Vasudevan and Sadananda [Vasudevan, Sadananda and Loaut (1993); Vasudevan and Sadananda (1995); Sadananda and Vasudevan (1997, 2004, 2005)]. The numerical models here reported could also be used to study the effect of internal stresses on the fatigue crack initiation at the notch tip [Kujawski and Stoychev (2007)]. Furthermore, the present work is preliminary to a more general research plan to investigate the possibility of lightening structural components by using opportunely coated – *i.e.* with the most suitable coating – aluminium or titanium alloys.

2 Material and experimental technique

The substrate material is Ti-6Al-4V ELI ASTM F136 with the following alloy composition (wt.%): 0.006 C, 3.800 V, 6.000 Al, 0.120 Fe, 0.099 O, 0.003 H, 0.009 N and Ti bal. The ultimate tensile strength and the yield strength of the material are, respectively, 895 MPa and 829 MPa, as certified by the dealer of the material. The standard specimens (ISO 1143) for fatigue testing were produced from bars with a 12-mm diameter. The minimum diameter was 8 mm and the wide fillet radius of the gage length was 40 mm (Fig. 1). Surface finishing operations within the gage length were accurately performed. The mechanical polishing allowed to keep the average surface roughness R_a below 0.20 μm . Circumferential notches were prevented by means of the final lengthwise polishing.

A 120° V-shaped notch was machined at the minimum cross section of one half of the specimens. It was 0.2 mm deep and transversal to the specimens axis. Hence, as depicted in Fig. 1, the notch size was very small if compared to the specimen cross section. The nominal bending stress to the notched specimens was then approximated to that of the smooth ones. A parameter characterizing the elastic stress amplification produced by the notch was evaluated by means of a preliminary

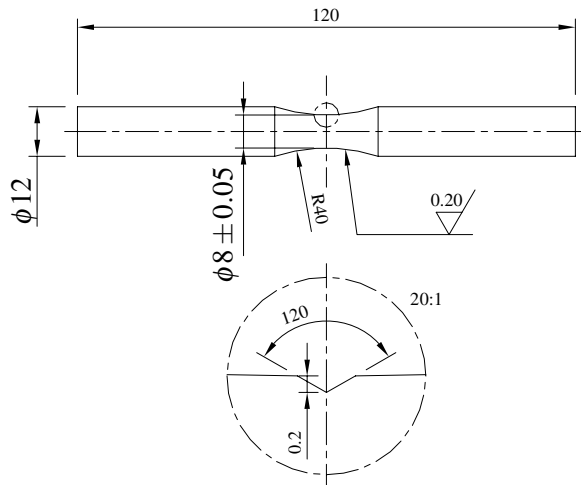


Figure 1: Dimensions of the specimens used in the fatigue tests

numerical model.

One half of the notched and smooth specimens were coated at LAFER Spa, Piacenza, Italy, with a commercial TiN arc-deposited PVD film. The film was deposited at a nominal temperature of 420°C and its average thickness was 3.9 μm . The bulk material Vickers microhardness was measured (Remet HX-1000 Vickers microindenter) at the Department of Materials and Environmental Engineering, University of Modena and Reggio Emilia, Modena, Italy, prior and after the deposition process for verifying if the mechanical properties had been affected by the deposition process temperature. The surface hardness of the alloy was $271 \pm 4 \text{ HV}_{0.5}$ before the deposition and $286 \pm 4 \text{ HV}_{0.5}$ afterwards [Baragetti, Lusvarghi, Pighetti Mantini and Tordini (2007)]. Therefore, the collected measurements suggested that no significant alterations in the substrate mechanical properties should occur after the heat treatment.

Rotating bending tests were performed ($R = -1$) on a computer-controlled machine (Italsigma X2TM412, Forlì, Italy) at a frequency of 50 Hz (3000 rpm) in laboratory air. Four series of fifteen specimens each were tested under fatigue with an upper limit of 200000 load cycles. The

series included smooth-uncoated, smooth-coated, notched-uncoated and notched-coated specimens. The statistical analysis procedure used to calculate the average value of the fatigue limit was the stair-case method (see the standard UNI 3964). The step chosen for the load variation was 20 MPa. Each bending stress level was set to the corresponding value of the maximum bending stress at the specimen minimum cross section without notch. The smooth-uncoated samples were loaded at maximum alternating stresses within the range 600-720 MPa, the smooth-coated within 540-640 MPa, the notched-uncoated within 300-360 MPa and the notched-coated within 260-300 MPa [Baragetti, Lusvarghi, Pighetti Mantini and Tordini (2007)].

A representative selection of fracture surfaces was observed using SEM (FEI Quanta-200) at the Department of Materials and Environmental Engineering, University of Modena and Reggio Emilia, Modena, Italy [Baragetti, Lusvarghi, Pighetti Mantini and Tordini (2007)]. A particular attention was given to the study of crack initiation sites.

3 Results and discussion

3.1 Fatigue test results

The differences in the above reported ranges of bending stress clearly indicate that the fatigue behaviour was influenced by both the presence of the coating and of the notch. The results [Baragetti, Lusvarghi, Pighetti Mantini and Tordini (2007)] of the rotating bending tests for each series of specimens are reported in Tabs. 1 to 4. Based on the experimental data, fatigue limit values of respectively 646 MPa for the smooth-uncoated material and 574 MPa for the coated one were calculated. A standard error of 45 MPa was estimated for the value of the fatigue limit for both series of specimens. Due to the notch, the fatigue limit decreased to 327 MPa for the uncoated material and to 281 MPa for the coated one, with standard errors of 14 MPa and 9 MPa respectively. From the experimental evidence, the fatigue test results were quite scattered, as far as the smooth specimens are concerned. On the con-

Table 1: Smooth-uncoated specimens: fatigue test results

Test no.	Bending stress, MPa	Number of cycles
1	720	31733
2	700	200000
3	720	22417
4	700	200000
5	720	52244
6	700	47978
7	680	35411
8	660	74609
9	640	200000
10	660	74609
11	640	154972
12	620	200000
13	640	56579
14	620	75245
15	600	200000
Fatigue limit, MPa		646
Standard error, MPa		45

Table 2: Smooth-coated specimens: fatigue test results

Test no.	Bending stress, MPa	Number of cycles
1	640	141207
2	620	200000
3	640	53042
4	620	48125
5	600	148690
6	580	66743
7	560	200000
8	580	200000
9	600	118347
10	580	118262
11	560	87067
12	540	200000
13	560	101545
14	540	200000
15	560	154570
Fatigue limit, MPa		574
Standard error, MPa		45

Table 3: Notched-uncoated specimens: fatigue test results

Test no.	Bending stress, MPa	Number of cycles
1	320	< 200000
2	300	200000
3	320	200000
4	340	129744
5	320	200000
6	340	139330
7	320	200000
8	340	133551
9	320	168142
10	300	200000
11	320	200000
12	340	200000
13	360	70778
14	340	112448
15	320	123004
Fatigue limit, MPa		327
Standard error, MPa		14

Table 4: Notched-coated specimens: fatigue test results

Test no.	Bending stress, MPa	Number of cycles
1	300	141232
2	280	200000
3	300	112700
4	280	200000
5	300	171742
6	280	188396
7	260	200000
8	280	186474
9	260	200000
10	280	200000
11	300	121931
12	280	200000
13	300	140712
14	280	170762
15	260	200000
Fatigue limit, MPa		281
Standard error, MPa		9

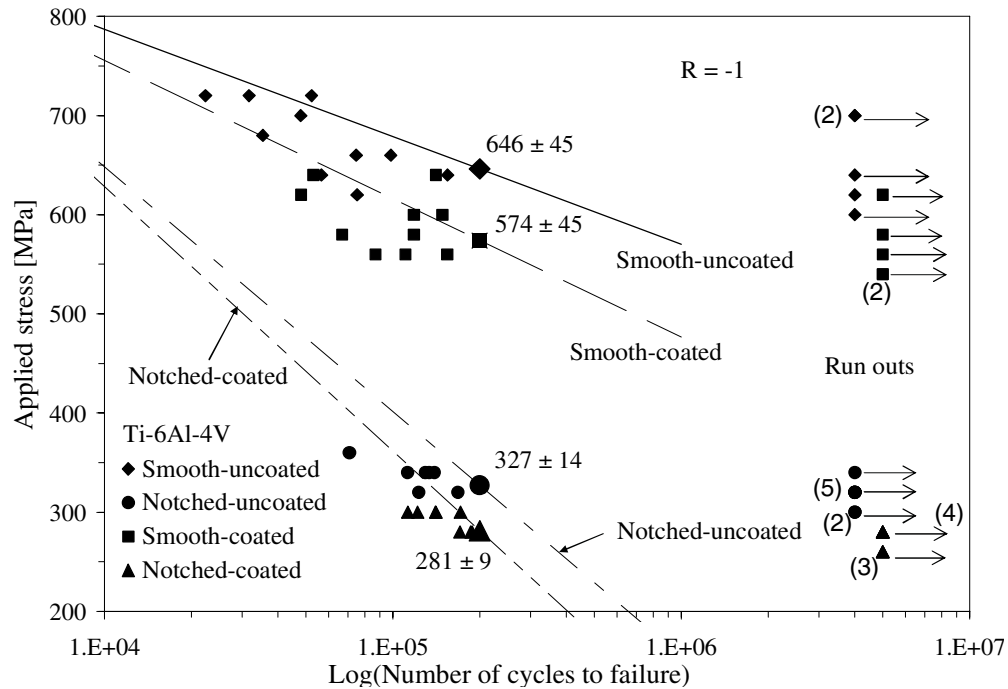


Figure 2: Applied stress vs. cycles to failure diagram

trary, the results obtained for the notched specimens presented a much lower dispersion. Indeed, the notch acted as a dominant stress concentrator with respect to all the other defects that may exist in the bulk material. However, the reliability of the experimental results for the smooth material was confirmed by the data available in the literature [American Society for Metals (1980)]. Fig. 2 summarizes the laboratory observations listed in Tabs. 1 to 4. Approximated S/N curves matching the data collected throughout the fatigue tests are also depicted in the finite life region of the Wöhler diagram. They were plotted by linking the boundary of quasi-static (10^3 cycles) failure to the calculated fatigue limit at 200000 load cycles.

These data show a small difference in the fatigue behaviour between the coated and the uncoated specimens. The coating produced a lowering in the average value of the fatigue limit by less than 12% for the smooth specimens and by 14% for the notched ones. Thus the presence of the TiN coating seemed to be little detrimental to the substrate fatigue properties. The percentages of decrease in the average fatigue limits show a similar behaviour between smooth-coated and notched-

coated specimens with respect to the uncoated ones. Only few references report data on the fatigue behaviour of TiN-coated Ti-6Al-4V and, from this point of view, no significant alteration was observed [Wilson, Leyland and Matthews (1999)].

A fatigue stress intensification factor K_f was used to represent the reduction in the fatigue limit of the notched titanium alloy. It is the ratio between the average fatigue limits at 200000 load cycles of the smooth and the notched specimens. The values for such a parameter are 1.98 for the uncoated specimens and 2.04 for the coated ones.

3.2 Numerical models

The numerical analyses were performed to understand and interpret the experimental results by evaluating the stress distribution underneath the surface at the minimum specimen cross section as well as the stress in the coating. Several 3D solid models were processed for both the smooth and notched specimens with the FE code ABAQUS 6.6-1[®]. The submodeling technique was also used for refining the calculation results over the minimum cross section and for specifying

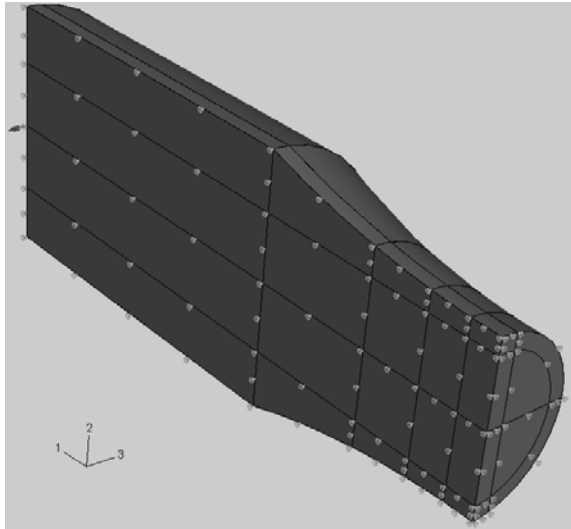


Figure 3: Boundary condition and load on a FE model reproducing a smooth specimen

ing the initial residual stress field induced by the PVD deposition process. Due to the specimen symmetry and to the way the bending load was applied, only a quarter of the complete geometry was modeled. The notch was modeled with an adequately rounded notch tip in order to match the corner radius of the insert tool used for machining. Suitable boundary conditions were imposed on the two planes of symmetry used to cut the specimen portion under consideration (Fig. 3). The uniform bending load condition along every specimen was imposed with a concentrated moment applied on the neutral axis of the cylindrical end free surface (see on the left side of Fig. 3). The coupling-kinematic option was used to traduce the rotation produced by the moment into the corresponding translations of the nodes lying on the end surface. Fig. 4 depicts the geometry of the general model for the notched-coated specimens and the embedded submodel, its location pointed at by the arrow.

The surface residual stress field was specified by introducing suitable prestress conditions into solid partitions produced in the coated specimen model. Such partitions were generated at the surface layer by offsetting the external free surface. Fig. 5 shows the partition of the same submodel depicted in Fig. 4. One of the mentioned parti-

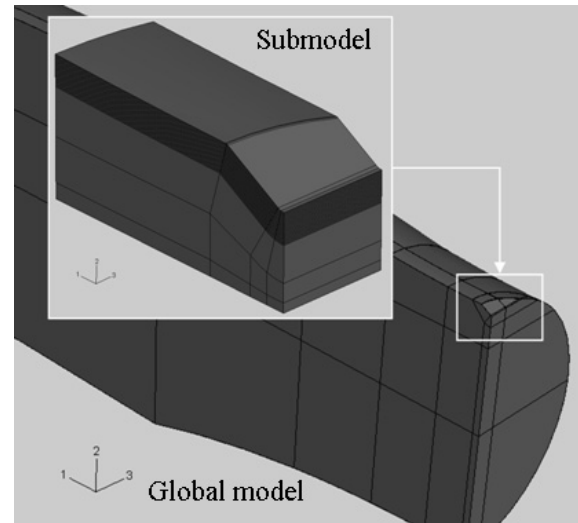


Figure 4: FE global model of a notched-coated specimen and particular of the related submodel

tions is shown in the figure. A typical and realistic distribution for the residual stresses oriented along the specimen axial direction (S11) was derived from the reference [Baragetti, La Vecchia and Terranova (2005)]. The high value of surface compression residual stresses makes it less important to know the exact trend of the residual stress field below the surface level. Indeed, numerical simulations demonstrated that the stress intensity factor range at different crack depths was not significantly affected by the input of different experimental trends of subsurface residual stresses [Baragetti, La Vecchia and Terranova (2005)]. Thus, the provided self equilibrated trend was used in the calculations also for the studied titanium alloy. The high surface compression residual stresses were reasonably assumed to be constant in the coating layer, while below the coating-substrate interface their moduli were dropped with a steep gradient. An inversion point is then reached moving towards the core of the bulk material and a tensile peak stress is then approached. The surface residual stress in the coating was conservatively set at -2400 MPa [Bemporad, Sebastiani, De Felicis, Carassiti, Valle and Casadei (2006); Baragetti, La Vecchia and Terranova (2005)], the inversion point at 0.02 mm below the substrate surface and the maximum tensile

value of 400 MPa at 0.04 mm. It is also important to remark that the modeled substrate material plasticizes under the combined actions of the external load and the residual stresses in the areas where maximum tensile and compression residual stresses are present. Therefore, the stresses produced in the specimen plasticized areas were lower than the ones that would arise in a perfectly elastic material. Verifications of the stress self-equilibrium condition were performed with good results after each analysis by comparing perfectly elastic and elastic-plastic models.

Eight-node C3D8 solid brick linear elements were selected to build up the meshes. Models and sub-models having more than 600000 dof were generated. Fig. 6 shows the mesh of a notched specimen submodel with the FE code visualization of the SS1 stress map after loading. The bending moment values used in the numerical models were set to produce bending stresses close to the fatigue limit levels from experimental tests on the uncoated specimens. The same bending moments were applied to the models reproducing both the coated and the uncoated specimens in order to enable the comparison of the results with and without coating. Hence, bending moments of 17 Nm for the notched specimens and 32 Nm for the smooth ones were considered. An elastic-perfectly plastic behaviour was adopted for the bulk material, while each coating was assumed to be perfectly elastic to reproduce its brittle nature. The von Mises' criterion was adopted to simulate the approaching of the yield condition. No failure criteria were adopted for the coating analysis. Four values of the coating elastic modulus were analysed for each model to verify the influence of such a parameter on the local stress state at the coating and at the interface with the bulk material. Elastic moduli of 100, 200, 300 and 400 GPa were studied. The TiN PVD coating analysed in this work should have an elastic modulus within the range 300-400 GPa [Mendibide, Steyer, Fontaine and Goudeau (2006); Puchi-Cabrera, Mat3nez, Herrera, Berr3os, Dixit and Bhat (2004)]. An investigation of this parameter was made to evaluate the best "bulk" mechanical behaviour that the designer of a coating should consider and try to

obtain for the final deposited product.

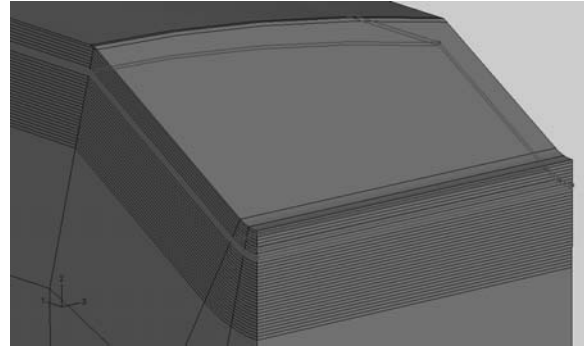


Figure 5: Partition of the surface layer of the sub-model shown in Fig. 4

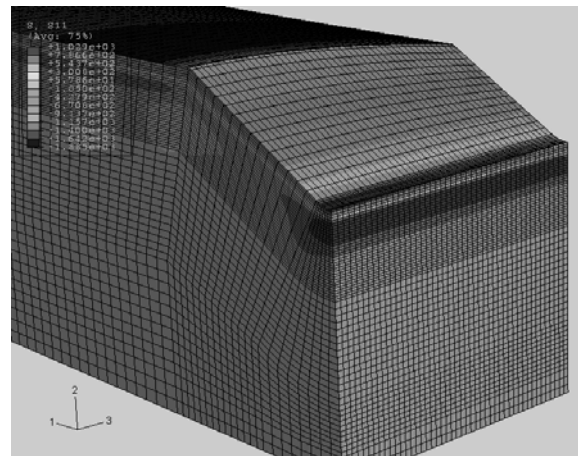


Figure 6: SS1 stress (MPa) map and mesh in a notched-coated specimen submodel

By means of a preliminary elastic analysis with the notched and smooth uncoated specimen models, the amplification stress coefficient for the notched specimens was evaluated. The solution provided a value of 3.70. This clearly gives rise to a local plasticization at the notch root. The comparison between this parameter with the much lower K_f from the tests indicates that the stress redistribution following the notch tip plasticization should play a fundamental role in the fatigue behaviour of the notched specimens [Haritos, Nicholas and Lanning (1999); Lanning, Haritos and Nicholas (1999)].

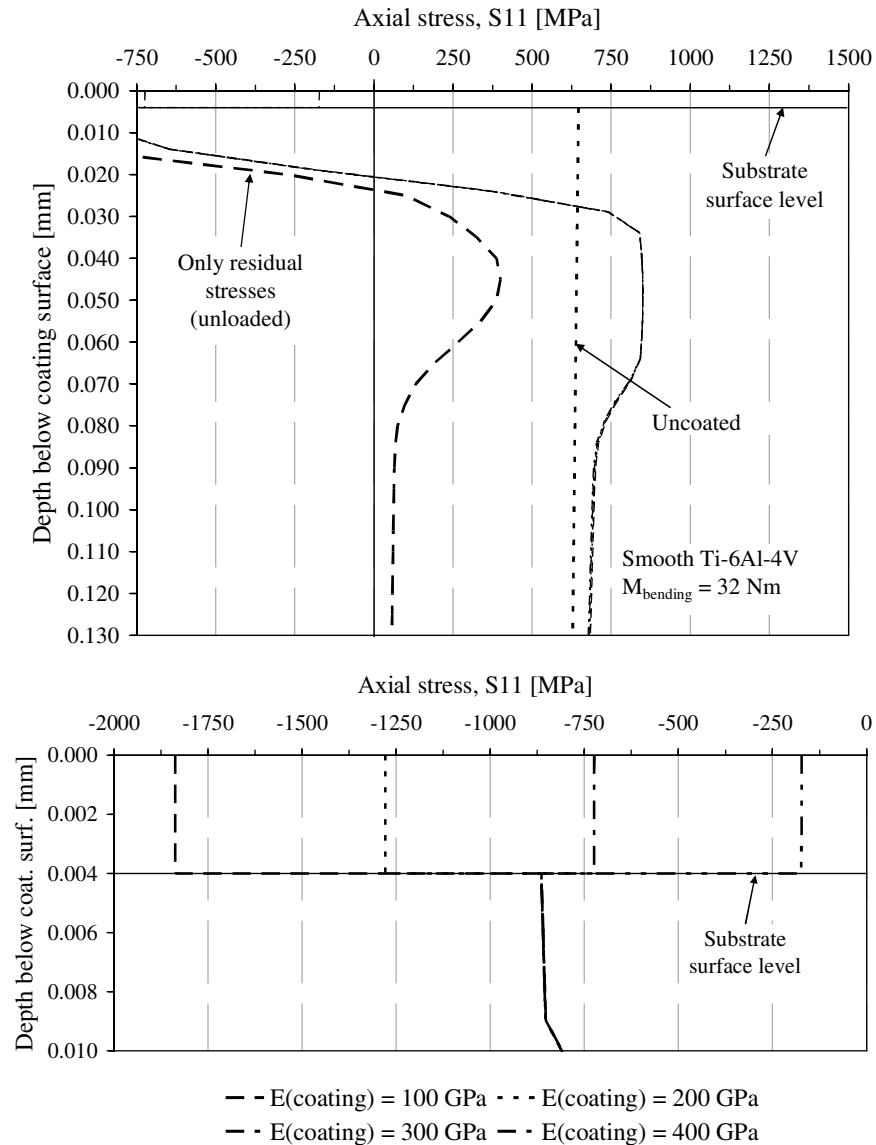


Figure 7: FEM results: S11 stress at the minimum cross section vs. depth below coating surface curves of the smooth specimen model with coatings having different elastic moduli and (below) a detail of the stress state in the coating

The main FEM results are plotted in the diagrams shown in Figs. 7 and 9. The curves for the S11 stress component over the minimum specimen cross section are plotted vs. the depth below the external surface. The self-equilibrated residual stress trend (unloaded model) in the presence of the coating is shown on each diagram left side. The minimum negative values are not present in the diagrams for a better visualization. At the bottom of each figure the curves after loading and the local stresses in the coating – for every coating

elastic modulus – are depicted.

The detail of the diagram in Fig. 7 shows that for loaded smooth specimens every coating is subjected to compression stresses, while the subsurface tensile stresses are greater than for the uncoated material and produce a localized material plasticization. Thus, with such a high surface compression stress, the coating would remain under compression at the tested fatigue load level even with the highest – and common for TiN PVD – elastic moduli. On the other hand, the tensile

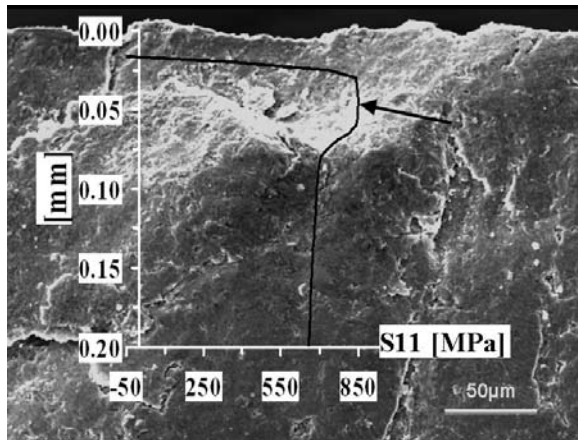


Figure 8: SEM micrograph of a coated smooth specimen. Superposition of the FEM stress gradient on the crack initiation site. The arrow points at the maximum tensile stress position in the initiation area

stresses in the coated bulk material are higher than the ones without coating and locally approach the yield strength. Also, the trends in the substrate are practically the same, independently of the coating elastic modulus. This parameter seems to influence only the local stress state at the coating. The surface compression stresses should prevent the coating cracking and keep possible defects before loading closed. On the contrary, the high tensile stresses reached underneath, and very close to the substrate surface, could justify the lowering in the fatigue limit observed for the coated specimens. As confirmed by SEM micrographs of coated specimen fracture surfaces [Baragetti, Lusvarghi, Pighetti Mantini and Tordini (2007)], fatigue cracks initiated near and below the substrate surface level and propagated giving rise to a net brittle fracture of the coating. Therefore, the studied titanium alloy could have developed subsurface cracks under fatigue in the area where the maximum tensile stresses took place. This behaviour could represent a problem also for fatigue lives exceeding 10^7 cycles [Haritos, Nicholas and Lanning (1999)], unless the tensile stress peak is dropped and pushed towards the bulk material core. Fig. 8 shows the superposition of the stress gradient with the 300-GPa coating and the fracture surface of a smooth-coated specimen: the

crack nucleation should have occurred where the calculated tensile stresses reach their maximum value (see arrow).

The analyses on the notched specimen model provided the results shown in Fig. 9. The stress gradient of the uncoated sample (Fig. 9, upper diagram) is no longer linear and it is affected by the local plasticization occurring at the notch tip. The trends for the substrate with different coating elastic moduli are nearly the same as for the smooth specimens. In this case the presence of the residual stress field translates the tensile stress peaks below the surface level without changing its modulus. Analogously to the smooth specimens, the FEM results fit well with the SEM observations of notched-coated specimen fracture surfaces, which show again subsurface crack initiations in the bulk material. A similar decrease in the fatigue behaviour to what happens with the smooth material may suggest that the subsurface position of maximum tensile stresses could play a fundamental role in the fatigue behaviour of a Ti-6Al-4V alloy, which could be even more important than the presence of a notch. Differently from the smooth specimen model, the stress amplification at the notch root gives rise to resultant tensile stresses in the coating having the higher elastic moduli, even if the compression stresses induced by PVD process contribute to limit the problem. The tensile stress calculated with the 400-GPa coating is 1650 MPa, while 850 MPa refers to the 300-GPa coating. The computed elastic E11 strains of the 300-GPa and the 400-GPa coatings are, respectively, 0.0022 and 0.0035. Such values could be close to the coating critical fracture strain [Shiozawa, Nishino and Handa (1992); Su, Yao, Wei, Kao and Wu (1999, Thin Solid Films)], even if, as afore said, SEM micrographs showed that the coating fracture might have not occurred before crack propagation. The stress in the coating is compressive for elastic moduli equal to 200 GPa and 100 GPa. This indicates that coatings having a lower rigidity could aid to prevent coating fracture under loading condition, provided that the residual stress distribution is similar to that of the more rigid ones.

FEM analyses showed that the residual stresses

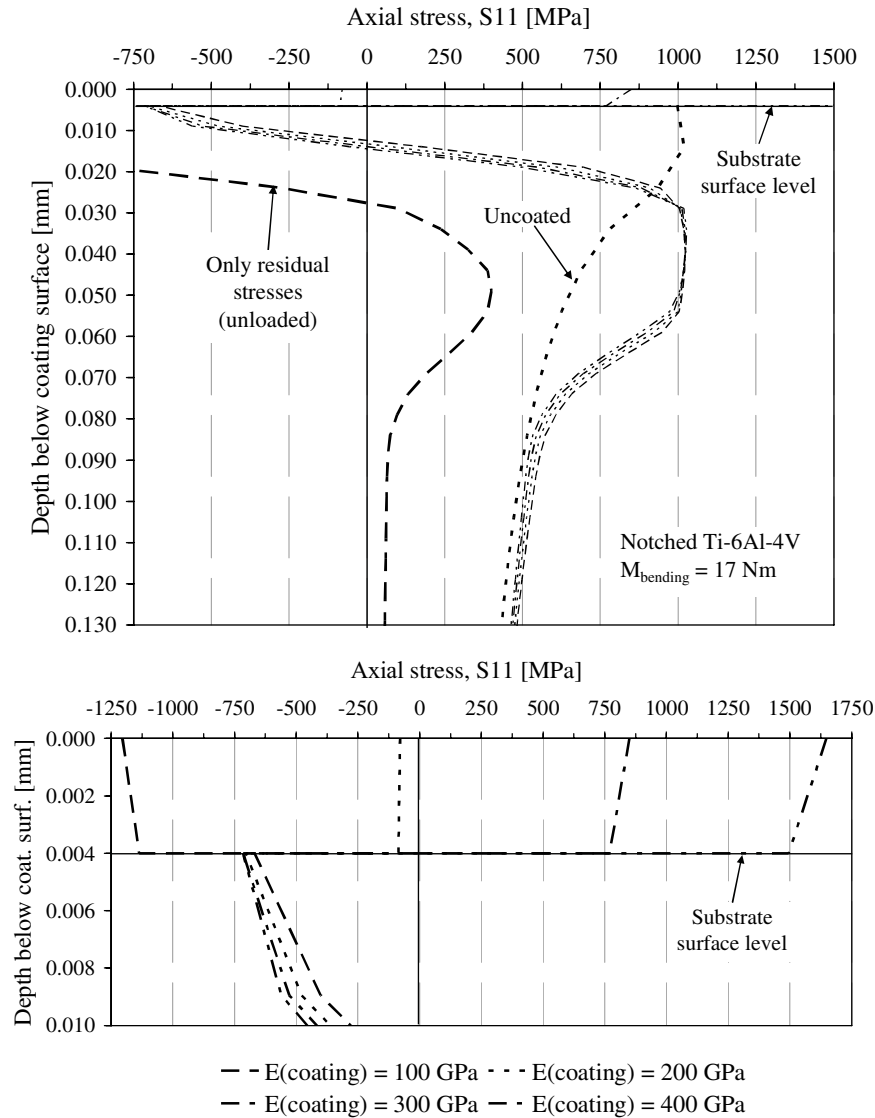


Figure 9: FEM results: S_{11} stress at the notch tip vs. depth below coating surface curves of the notched specimen model with coatings having different elastic moduli and (below) a detail of the stress state in the coating

induced by the coating deposition process generate similar stress trends between smooth and notched specimens in the bulk material after loading. The experimental tests evidenced that the presence of the coating was similarly detrimental – *i.e.* with a similar percentage of decrease – for both the smooth and notched specimens. In each model the maximum tensile stresses are shifted below the surface level and generate local plasticization. The high surface compression stresses should prevent any crack nucleation in the area. Thus, an explanation for the fatigue behaviour ob-

served with the tests may be found in the subsurface crack nucleation, which the calculated resultant stress trends could make it possible in both types of specimen.

4 Summary

The fatigue tests performed on a TiN PVD-coated and uncoated – notched and smooth – Ti-6Al-4V titanium alloy pointed out that the coating was little detrimental to the base material fatigue resistance. The notched and the smooth specimens

had a similar reduction in the fatigue life within the range of 12-14%. Such behaviour fits well with FEM calculations, which provided similar resultant stress trends for both the notched-coated and smooth-coated specimen models. Thus, as regards the bulk material, the coating deposition seems to limit the notch effect, making it possible to get the same results with both notched and smooth material. Furthermore, the maximum tensile stresses shifted below the surface could justify the nucleation of subsurface cracks that likely occurred in the bulk material. Especially for notched components, with the coating deposition a valuable benefit could be achieved for the improvement of the wear resistance properties combined with a limited lowering of the fatigue limit.

Defects in the brittle TiN coating can easily generate through-thickness cracks, which represent severe micro-notches for the substrate [Shiozawa, Nishino and Handa (1992)], and are hence detrimental for its fatigue resistance. FEM analyses showed resultant tensile stresses in the coating after loading for the notched specimen model with 300 and 400-GPa coating elastic moduli. Such stresses keep the cracks open, making the less rigid coatings that were considered in the computations more attractive from this point of view. Compression stresses may also prevent coating fracture from occurring.

Numerical results indicate that the application of TiN PVD on Ti-6Al-4V substrate may prevent the nucleation of surface cracks, even if the subsurface tensile stress may be unbeneficial. For fatigue lives at higher numbers of cycles, *i.e.* at lower load levels, the coating analysed should be more effective. The coating strain would be reduced – that is particularly beneficial for the notched material – and so even the maximum subsurface tensile stresses.

Acknowledgement: The Authors would like to thank prof. A.K. Vasudevan for the discussion and for his precious suggestions, LAFER, Piacenza, Italy, for the execution of the coatings and the Department of Materials and Environmental Engineering, University of Modena and Reggio Emilia, Modena, Italy, for the SEM observations.

References

- American Society for Metals** (1980): Metals Handbook, Properties and Selection: Stainless Steels, Tool Materials and Special-Purpose Metals, 9th Ed., vol. 3, ASM, Metals Park, Ohio, pp. 388-391.
- Baragetti, S.; La Vecchia, G. M.; Terranova, A.** (2003): Fatigue behaviour and FEM modelling of thin-coated components. *Int J Fat*, vol. 25, pp. 1229-1238.
- Baragetti, S.; La Vecchia, G. M.; Terranova, A.** (2005): Variables affecting the fatigue resistance of PVD-coated components. *Int J Fat*, vol. 27(10-12), pp. 1541-1550.
- Baragetti, S.** (2007): Fatigue resistance of steel and titanium PVD coated spur gears. *Int J Fat*, vol. 29, pp. 1893-1903.
- Baragetti, S.; Lusvardi, L.; Pighetti Mantini, F.; Tordini, F.** (2007): Fatigue Behaviour of Notched PVD-coated Titanium Components. *Key Engineering Materials*, vols. 348-349, pp. 313-316.
- Bemporad, E.; Sebastiani, M.; De Felicis, D.; Carassiti, F.; Valle, R.; Casadei, F.** (2006): Production and characterization of duplex coatings (HVOF and PVD) on Ti-6Al-4V substrate. *Thin Solid Films*, vol. 515, pp. 186-194.
- Gelfi, M.; La Vecchia, G. M.; Lecis, N.; Troglio, S.** (2005): Relationship between through thickness residual stress of CrN-PVD coatings and fatigue nucleation sites. *Surf Coat Technol*, vol. 192, pp. 263-268.
- Guu, Y. H.; Hocheng, H.** (2001): Improvement of fatigue life of electrical discharge machined AISI D2 tool steel by TiN coating. *Mater Sci Eng*, vol. A318, pp. 155-162.
- Haritos, G. K.; Nicholas, T.; Lanning, D. B.** (1999): Notch size effects in HCF behavior of Ti-6Al-4V. *Int J Fat*, vol. 21, pp. 643-652.
- Kato, M.; Deng, G.; Inoue, K.; Takatsu, N.** (1993): Evaluation of the strength of carburized spur gear teeth based on fracture mechanics. *JSME Int J - Series C*, vol. 36(2), pp. 233-240.
- Kim, K. R.; Suh, C. M.; Murakami, R. I.; Chung, C. W.** (2003): Effect of intrinsic prop-

erties of ceramic coatings on fatigue behaviour of Cr-Mo-V steels. *Surf Coat Technol*, vol. 171, pp. 15-23.

Kolkman, H. J. (1995): Effect of TiN/Ti gas turbine compressor coatings on the fatigue strength of Ti-6Al-4V base metal. *Surf Coat Technol*, vol. 72, pp. 30-36.

Kujawski, D.; Stoychev, S. (2007): Internal stress effects on fatigue crack initiation at notches. *Int J Fat*, vol. 29, pp. 1744-1750.

Lanning, D. B.; Haritos, G. K.; Nicholas, T. (1999): On the use of critical distance theories for the prediction of the high cycle fatigue limit stress in notched Ti-6Al-4V. *Int J Fat*, vol. 27, pp. 45-57.

Lanning, D. B.; Nicholas, T.; Haritos, G. K. (2005): Influence of stress state on high cycle fatigue of notched Ti-6Al-4V specimens. *Int J Fat*, vol. 21, pp. S87-S95.

Mendibide, C.; Steyer, P.; Fontaine, J.; Goudeau, P. (2006): 4124 Improvement of the tribological behaviour of PVD nanostratified TiN/CrN coatings – An explanation. *Surf Coat Technol*, vol. 201, pp. 4119-4124.

Merlo, A. M. (2003): The contribution of surface engineering to the product performance in the automotive industry. *Surf Coat Technol*, vols. 174-175, pp. 21-26.

PalDey, S.; Deevi, S. C. (2003): Single layer and multilayer wear resistant coatings of (Ti,Al)N: a review. *Mater Sci Eng*, vol. A342, pp. 58-79.

Puchi-Cabrera, E. S.; Matínez, F.; Herrera, I.; Berríos, J. A.; Dixit, S.; Bhat, D. (2004): On the fatigue behavior of an AISI 316L stainless steel coated with a PVD TiN deposit. *Surf Coat Technol*, vol. 182, pp. 276-286.

Sadananda, K.; Vasudevan, A. K. (1997): Short crack growth and internal stresses. *Int J Fat*, vol. 19, pp. S99-S109.

Sadananda, K.; Vasudevan, A. K. (2004): Non-propagating incipient cracks from sharp notches under fatigue. *Acta Mater*, vol. 52(14), pp. 4239-4249.

Sadananda, K.; Vasudevan, A. K. (2005): Fatigue crack growth behavior of titanium alloys. *Int*

J Fat, vol. 27(10-12), pp. 1255-1266.

Shiozawa, K.; Nishino, S.; Handa, K. (1992): The influence of applied stress ratio on fatigue-strength of TiN-coated carbon-steel. *JSME Int J - Series I*, vol. 35(3), pp. 347-353.

Su, Y. L.; Yao, S. H.; Wei, C. S.; Wu, C. T.; Kao, W. H. (1998): Evaluation on wear, tension and fatigue behaviour of various PVD coated materials. *Mater Lett*, vol. 35, pp. 255-260.

Su, Y. L.; Yao, S. H.; Wei, C. S.; Kao, W. H.; Wu, C. T. (1999): Comparison of wear, tensile, and fatigue properties of PVD coated materials. *Mater Sci Technol*, vol. 15(1), pp. 73-77.

Su, Y. L.; Yao, S. H.; Wei, C. S.; Kao, W. H.; Wu, C. T. (1999): Influence of single- and multilayer TiN films on the axial tension and fatigue performance of AISI 1045 steel. *Thin Solid Films*, vol. 338, pp. 177-184.

Vasudevan, A. K.; Sadananda, K. (1995): Classification of fatigue crack growth behavior. *Met Trans A*, vol. 26A, pp. 1221-1234.

Vasudevan, A. K.; Sadananda, K.; Loaut, N. (1993): Two critical stress intensities for threshold crack propagation. *Scripta Metall*, vol. 28, pp. 65-70.

Vetter, J.; Barbezat, G.; Crummenauer, J.; Avissar, J. (2005): Surface treatment selections for automotive applications. *Surf Coat Technol*, vol. 200, pp. 1962-1968.

Wilson, A. D.; Leyland, A.; Matthews, A. (1999): A comparative study of the influence of plasma treatments, PVD coatings and ion implantation on the tribological performance of Ti-6Al-4V. *Surf Coat Technol*, vol. 114, pp. 70-80.